45 Tamir I, Cambier JC. Antigen receptor signaling: integration of protein tyrosine kinase functions. *Oncogene* 1998; **11**: 1353–64.
46 Downward J. Ras signalling and apoptosis. *Curr Opin Genet Dev* 1998; **8**: 49–54.
47 Miyake I, Hakomori Y, Misu Y *et al.* Domain-specific function of ShcC docking protein in neuroblastoma cells. *Oncogene* 2005; **24**: 3206–15.
48 Bresler SC, Wood AC, Haglund EA *et al.* Differential inhibitor sensitivity of anaplastic lymphoma kinase variants found in neuroblastoma. *Sci Transl Med* 2011; **3**: 108ra14.

Supporting Information

Additional Supporting Information may be found in the online version of this article:

Fig. S1. Relative Shf expression profiles in favorable/unfavorable samples.

Fig. S2. Tissue and cell line specificities of Shf and anaplastic lymphoma kinase (ALK).

doi: 10.1111/cas.12115

Oncogene (2013), 1–9

www.nature.com/onc

ORIGINAL ARTICLE

RUNX3 interacts with MYCN and facilitates protein degradation in neuroblastoma

F Yu[1,2,3], W Gao[1,4], T Yokochi[1], Y Suenaga[1], K Ando[1], M Ohira[5], Y Nakamura[1] and A Nakagawara[1,2]

RUNX3, a runt-related transcription factor, has a crucial role in dorsal root ganglion neurogenesis. Recent studies have suggested that RUNX3 acts as a tumor suppressor in stomach, colon and breast cancer. However, the biological role of RUNX3 in neuroblastoma remains elusive. Here we report that high levels of *RUNX3* expression contribute to the favorable outcome in patients with neuroblastoma, whereas low levels of *RUNX3* expression result in poor outcome. Array-based analysis suggested that the allelic loss at chromosome 1p36 is one of the reasons why expression of *RUNX3* is downregulated in advanced neuroblastomas. Interestingly, the several patients survived from neuroblastoma with both high mRNA expressions of *MYCN* and *RUNX3*, suggesting that *RUNX3* high expression might overcome the aggressive behavior of *MYCN*. Exogenous expression of *RUNX3* strongly inhibits cell proliferation and migration in neuroblastoma cell lines. Furthermore, RUNX3 reduces the stability of MYCN protein in *MYCN*-amplified neuroblastoma cell lines, and this RUNX3-mediated MYCN degradation may depend on the physical interaction between RUNX3 and MYCN. Thus, our findings provide a tumor-suppressing mechanism by which RUNX3 inhibits the MYCN activity in neuroblastoma.

Oncogene advance online publication, 15 July 2013; doi:10.1038/onc.2013.221

Keywords: RUNX3; MYCN; neuroblastoma; tumor suppressor

INTRODUCTION

Human neuroblastoma, a neoplasm of peripheral neural crest origin, is the most common extracranial solid tumor of childhood and accounts for 15% of cancer deaths in children.[1,2] Despite recent advances in treatment options, aggressive neuroblastoma remains refractory to current therapy. The overall 5-year survival rate for patients with advanced-stage of neuroblastoma is 30–40%.[3–5] Neuroblastoma patients harboring genomic *MYCN* amplification accompanied by allelic deletion of short arm of chromosome 1 are at high risk for unfavorable outcome. Amplification of the proto-oncogene *MYCN* occurs in up to 25% of neuroblastoma, strongly correlating to the advanced-stage disease and the failure of chemotherapy treatment.[6–8] Loss of heterozygosity at 1p36 is found in 20–40% of neuroblastoma cases and is independently associated with progression-free survival. Thus, it has been predicted that candidates of tumor-suppressor gene may exist in this region.[9–11]

RUNX3 belongs to the Runt-related gene family, whose members are pivotal regulators of neuronal development.[12,13] *RUNX3* is located at human chromosome 1p36 and its gene product acts as a tumor suppressor in various cancers[14–18] except neuroblastoma. A possible role of RUNX3 in neuroblastoma is suggested by its transcriptional regulation of *TrkB*, which was identified as an oncogene.[19–22] Although the most neuroblastoma cell lines do not synthesize RUNX3 protein at detectable levels, exogenous expression of *RUNX3* causes the cell death, cell cycle arrest or differentiation in neuroblastoma.[23] In this study, we quantitatively measured the expression levels of *RUNX3* in 110 primary neuroblastoma samples to test the hypothesis that the inactivation of *RUNX3* is independently prognostic for adverse stages of the disease. Based on clinical analyses, investigation *in vitro* revealed a reliable mechanism by which RUNX3 inhibits the stability and oncogenic activity of MYCN in neuroblastoma.

RESULTS

Decreased expression of *RUNX3* is associated with poor prognosis in neuroblastoma patients

As the *RUNX3* gene is mapped to chromosome 1p36.2, which is frequently deleted in unfavorable neuroblastomas as well as other cancers, we asked whether *RUNX3* could act as a tumor-suppressor gene in neuroblastoma. We then examined the expression levels of *RUNX3* mRNA in 16 favorable (stage 1 or 2, single copy of *MYCN* and high expression of *TrkA*) and 16 unfavorable (stage 3 or 4, amplification of *MYCN* and low expression of *TrkA*) neuroblastoma samples by semiquantitative reverse transcription–PCR (RT–PCR).[24–27] *RUNX3* was expressed at higher levels in the favorable group than the unfavorable group (Figure 1a). This result prompted us to quantitatively measure the expression levels of *RUNX3* in 110 primary samples of neuroblastomas utilizing real-time PCR. We found that *RUNX3* expression levels in stage 1 and 2 patients tended to be higher (Figure 1b). To further understand the impact of *RUNX3* expression on patients outcome, we divided the clinical samples into two, such as *RUNX3* high ($n = 22$) and low ($n = 88$) expression groups, based on the mean value of *RUNX3* expression. Kaplan–Meier analysis showed that decreased expression of *RUNX3* mRNA was significantly correlated with poor survival rate ($P = 0.016$, Figure 1c). In addition, the possible

[1]Division of Biochemistry and Innovative Cancer Therapeutics, Chiba Cancer Center Research Institute, Chiba, Japan; [2]Department of Molecular Biology and Oncology, Chiba University Graduate School of Medicine, Chiba, Japan; [3]Department of Thoracic Surgery, Forth Hospital of Hebei Medical University, Hebei, PRC; [4]Department of First Surgery, Forth Hospital of Hebei Medical University, Hebei, PRC and [5]Division of Cancer Genomics, Chiba Cancer Center Research Institute, Chiba, Japan. Correspondence: Dr A Nakagawara, Chiba Cancer Center Research Institute, 666-2 Nitona, Chuo, Chiba 260-8717, Japan.
E-mail: akiranak@chiba-cc.jp
Received 10 February 2013; revised 24 April 2013; accepted 3 May 2013

relationship between *RUNX3* expression levels and various clinical and biological features from these samples were examined and summarized in Supplementary Table 1. Significantly high levels of *RUNX3* expression were found in the low-risk tumors (stages 1, 2 and 4s, $P<0.001$). Statistical correlation was also detectable between *RUNX3* expression and the copy number of *MYCN* ($P=0.047$). The log-rank test demonstrated that several prognostic factors, including *RUNX3*, were significantly correlated with

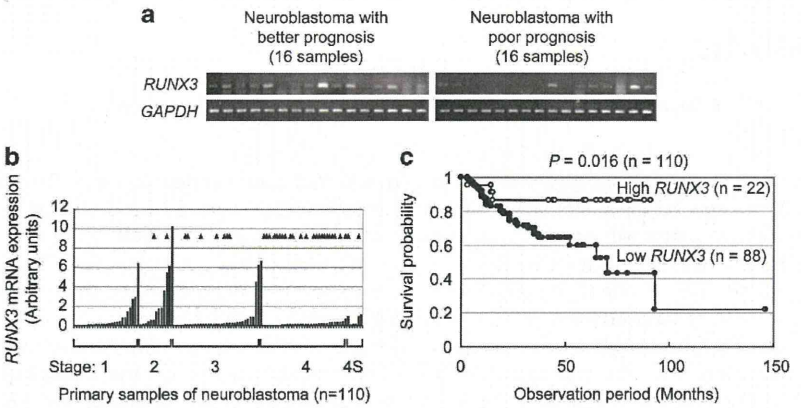

Figure 1. Expression levels of *RUNX3* in primary neuroblastomas. (**a**) Semi-quantitative RT–PCR analysis. Total RNA was prepared from primary samples with better prognosis (stages 1 and 2, *MYCN* single copy, $n=16$) and those with poor prognosis (stages 3 and 4, *MYCN* amplified, $n=16$). RT–PCR was performed to examine the expression levels of RUNX3. Glyceraldehyde 3-phosphate dehydrogenase (GAPDH) is employed for loading control. (**b**) Quantitative real-time PCR analysis. The relative expression levels of *RUNX3* in primary samples (stage 1, 2, 3, 4, and 4S) are shown. *RUNX3* levels were standardized using the corresponding *GAPDH* value of each neuroblastoma sample. Filled triangles indicate fatal cases due to neuroblastoma cancer. (**c**) Kaplan–Meier survival curves of patients with neuroblastoma. Expression levels of *RUNX3* in 110 primary neuroblastoma samples determined by real-time PCR were classified into two categories, such as high (open circle, $n=22$) and low (filled circle, $n=88$) expression groups, based on the mean value of *RUNX3* expression levels.

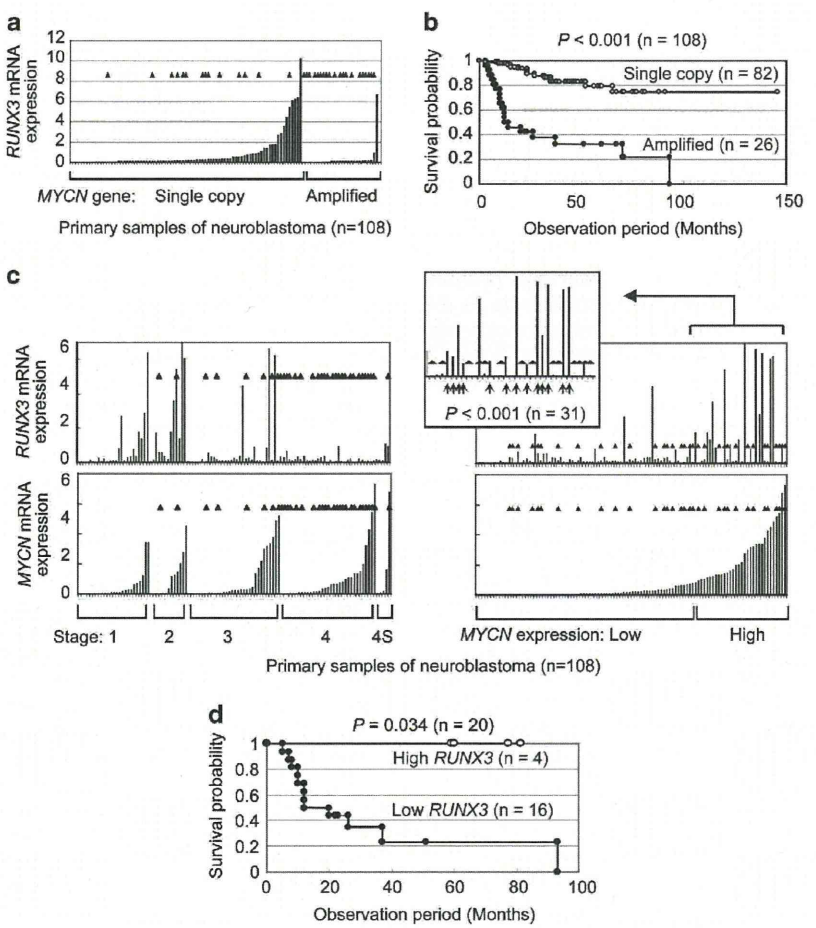

clinical outcome in these 110 neuroblastoma patients (Supplementary Table 2). The multivariate Cox regression analysis showed that *RUNX3* mRNA expression levels are not significantly associated with patient's survival only when International Neuroblastoma Staging System stages or *MYCN* copy number is employed (models C and E in Supplementary Table 3), suggesting that *RUNX3* expression levels are associated with these two factors in terms of patients' survivals.

The relationship between chromosomal deletion at 1p36 and expression of *RUNX3*

As low expression of *RUNX3* is correlated with poor patient's outcome, we sought to identify the possible mechanism underlying the suppression of *RUNX3* expression. According to the data obtained from array-comparative genomic hybridization analysis using UCSF BAC array (2464 BACs, ~1 Mb resolution), among 59 samples that were identified as diploid tumors, 12 tumors revealed to have a partial deletion at chromosome 1p36 (Supplementary Table 4), indicating that *RUNX3* expression is significantly lower in the tumor cells with 1p36 loss than those without the loss. These results suggest that the gene dosage effect is one of the reasons why *RUNX3* expression is decreased in aggressive neuroblastomas.

The outcome relationship between *RUNX3* and *MYCN* expressions in neuroblastoma patients

As we mentioned above, amplification of *MYCN* was significantly associated with low expression of *RUNX3*. A real-time PCR assay quantitatively measuring the expression levels of *RUNX3* also supported this notion (Figure 2a), as a majority of *RUNX3* high expression cases was observed in the tumors with single copy of *MYCN*. Consistent with previous literatures,[28] amplified *MYCN* is apparently related to fatal cases indicated by filled triangles in Figure 2a. Indeed, the Kaplan–Meier survival plot clearly demonstrated that the patients with amplified copies of *MYCN* die more quickly than those with a single copy (Figure 2b). These results lead us to the hypothesis that amplified copies of *MYCN* gene induce higher level of *MYCN* mRNA expression and high MYC pathway activity, resulted in death of neuroblastoma patients in which *RUNX3* is expressed in a low level. To test this possibility, the expression levels of *MYCN* in the primary neuroblastoma samples were quantitatively measured by a real-time PCR and were compared with *RUNX3* levels (Figure 2c). Nearly all tumors in stage 4 were fatal cases (shown by filled triangles in Figure 2c) and were associated with higher *MYCN* and lower *RUNX3* expressions (Figure 2c, left panels). In contrast, survivals were enriched in lower International Neuroblastoma Staging System stages (1 and 2) and were generally accompanied by lower *MYCN* and higher *RUNX3* expressions. Next, the primary neuroblastoma samples were arranged according to the expression levels of *MYCN* to further elucidate the correlation between *MYCN* and *RUNX3* expressions (Figure 2c, right panels). Primary samples were classified into two groups using the mean value of MYCN as the cutoff value. We found that, among the *MYCN* high-expression group, patients with higher expression levels of *RUNX3* tend to survive, whereas those with low expression died (Figure 2c, inset in right panels). Kaplan–Meier plot of the primary samples in which *MYCN* is highly expressed also supports this notion (Figure 2d). This result suggests that *RUNX3* high expression is closely associated with survival possibility of neuroblastoma patients, even though some of them expressed high level of *MYCN*.

The biological function of RUNX3 in neuroblastoma cells

The clinical study above promoted us to further investigate the function of RUNX3 in neuroblastoma cell lines. SK-N-BE

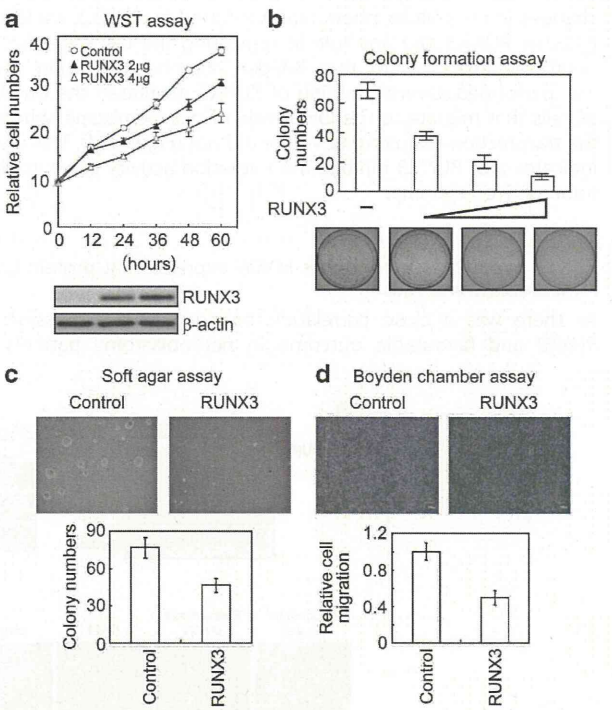

Figure 3. Transient transfection of RUNX3 suppresses the growth and migration of neuroblastoma cells. (**a**) WST assay. Empty vector or increasing amounts of RUNX3 expression plasmid were transfected into SK-N-BE cells. Cell growth was measured at indicated hours. The expression of exogenous RUNX3 was shown by immunoblotting (bottom panels). (**b**) Colony formation assay. SK-N-BE cells were transfected with increasing amounts of RUNX3 expression plasmid (0.5, 1 and 2 μg). Total amounts of plasmid DNA per transfection were kept constant (2 μg) with empty vector. The histograms represent the number of colonies in each group. Representative colony formation images are also shown. (**c**) Soft agar assay. SK-N-BE cells were transfected by either mock or RUNX3-expression vector. The cells were seeded onto soft agar plates in triplicate. The histograms represent the number of colonies (diameters > 300 μm) in each plate. Representative colony images are also shown. (**d**) Boyden chamber assay. Empty vector or RUNX3 expression plasmid was transfected into SK-N-BE cells. Numbers of migrated cells were counted and are represented as relative values. Control group was set to 1. Error bars represent the standard deviation obtained from triplicate experiments.

Figure 2. Inverse correlation between *RUNX3* and *MYCN* expression. Filled triangles shown in each panel indicate fatal cases due to neuroblastoma cancer. (**a**) Quantitative real-time PCR of *RUNX3* expression. Primary samples are classified into two groups based on the copy number of *MYCN* gene (single copy or amplified). (**b**) Kaplan–Meier survival plot according to a copy number of *MYCN*. A total of 108 primary neuroblastomas were classified into two categories (single or amplified). (**c**) The expression levels of *RUNX3* (top panels) and *MYCN* (bottom panels). Primary neuroblastoma samples are arranged according to stages (left panels) or relative *MYCN* expression values (right panels). *RUNX3* expression levels associated with high expression levels of *MYCN* are shown in detail (inset). Arrowheads indicate the survivals in which both *RUNX3* and *MYCN* were highly expressed. (**d**) Kaplan–Meier survival plot according to *RUNX3* expression levels. Twenty primary neuroblastomas in which *MYCN* is highly expressed were classified into two categories, such as high (open circle, $n = 4$) and low (filled circle, $n = 16$) *RUNX3* expression groups, based on the mean value of *RUNX3* expression levels.

(*MYCN* amplified) cells were transiently transfected with empty vector or increasing amounts of RUNX3 expression vector and the cell growth was examined by WST (water soluble tetrazolium salts) assay and colony formation assay. RUNX3 overexpression decreased the growth rate in a dose-dependent manner (Figure 3a). Similar results were obtained by conventional colony formation assay (Figure 3b). Furthermore, colony formation assay utilizing soft agar demonstrated that overexpression of RUNX3 decreased anchorage-independent cell growth, suggesting that RUNX3 could inhibit the oncogenic property of neuroblastoma-derived cell line (Figure 3c). In order to better understand the changes in the cellular phenotype mediated by RUNX3, we tested whether RUNX3 had any role in regulating the cell migration of neuroblastoma. Toward this, Boyden chamber migration assay was performed. Overexpression of RUNX3 decreased the number of cells that migrate to the lower side of the membrane, whereas the transfection of an empty vector did not (Figure 3d). This result indicates that RUNX3 inhibits the migration activity of neuroblastoma-derived cell line.

RUNX3 overexpression reduces MYCN expression at protein level in neuroblastoma cells

As there was a close correlation between high expression of *RUNX3* and favourable outcome in neuroblastoma patients in which *MYCN* is highly expressed, we hypothesized that RUNX3 may negatively regulate *MYCN* oncogenic activities, resulting in survival of neuroblastoma patients. Thus, we examined whether RUNX3 could control MYCN expression at either mRNA or protein level. Overexpression of RUNX3 decreased the MYCN proteins in a dose- and time-dependent manner (Figure 4a, left panels and Figure 4b), whereas RT–PCR showed that the mRNA expression level of *MYCN* was not affected by the exogenous *RUNX3* overexpression (Figure 4a, right panels). Essentially, similar results were obtained utilizing another *MYCN*-amplified neuroblastoma cell line NLF. These data indicate that RUNX3 reduced the expression of MYCN at protein level rather than mRNA level, suggesting that RUNX3 negatively regulates MYCN expression by the post-translational mechanism. Immunofluorescence microscopy demonstrated that the cells in which exogenous RUNX3 (red) was overexpressed showed less degree of endogenous MYCN (green; Figure 4c, top panels), indicating that exogenous RUNX3 and endogenous MYCN are mutually exclusive in terms of the protein expression pattern. We further examined the number of cells that have different expression patterns of RUNX3 and MYCN. Majority of the cells show either MYCN or RUNX3 expressions, and less than 10% of cells express both or none (Figure 4c, bottom panel). These results demonstrated that, at protein level, MYCN is inversely correlated with RUNX3 expression. In order to investigate reduction of MYCN protein in detail, the

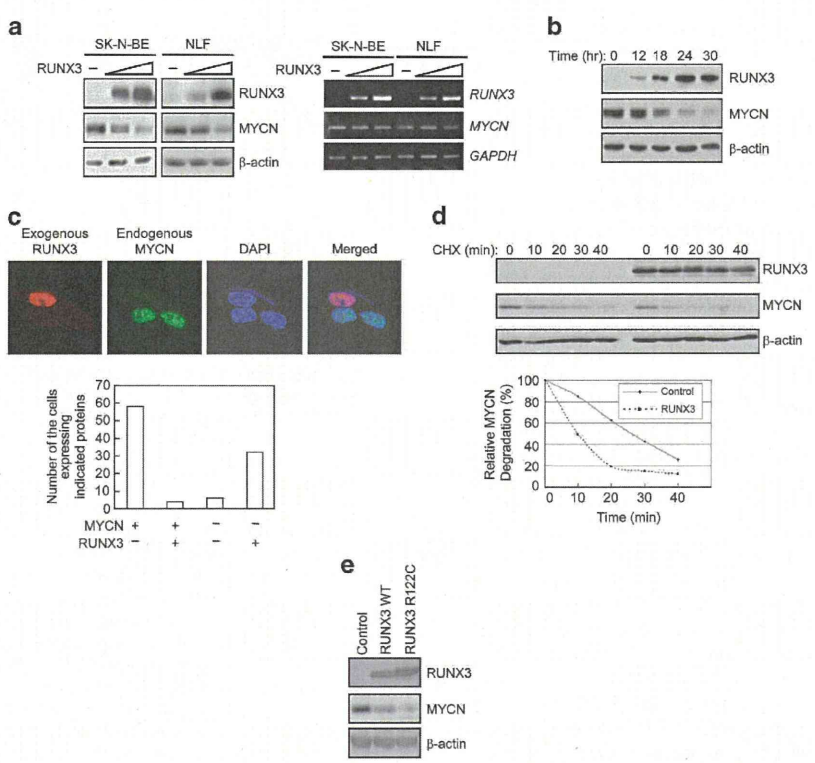

Figure 4. RUNX3 overexpression reduces the protein level of MYCN in neuroblastoma cells. (**a**) RUNX3 inhibits MYCN expression at protein level. SK-N-BE and NLF cells were transfected with empty vector or increasing amounts of RUNX3-expressing plasmid. Whole-cell lysates and total RNA were subjected to immunoblotting (IB; left panels) or RT–PCR (right panels), respectively. Actin and *GAPDH* were used as loading controls. (**b**) Time course. SK-N-BE cells were transfected with RUNX3-expressing plasmid. Cell lysates were prepared at indicated time points and were subjected to IB. (**c**) The subcellular localization of RUNX3 and MYCN are detected by immunofluorescent staining in SK-N-BE cells. Exogenous RUNX3 and endogenous MYCN were stained by anti-MYC tag (red) or anti-MYCN (green) antibodies, respectively. Nucleus was visualized by 4′-6-diamidino-2-phenylindole (DAPI) staining. The histogram represents the number of cells expressing indicated genes ($n = 100$). (**d**) RUNX3 decreases the half-life of MYCN. Empty vector or RUNX3-expressing plasmid was transfected into SK-N-BE cells, and the cells were treated with cycloheximide (CHX) and harvested at the indicated time points. A measure of 40 μg (the cells transfected with empty vector) or 60 μg (the cells with RUNX3 expression vector) of the cell lysate was employed, respectively. (**e**) MYCN degradation mediated by wild-type RUNX3 and transcriptionally deficient mutant RUNX3-R122C. SK-N-BE cells were transfected with empty vector, RUNX3 or point-mutated RUNX3-R122C-expressing plasmid.

degradation rate of endogenous MYCN in the absence or presence of RUNX3 was compared. Cycloheximide was used to inhibit the synthesis of new MYCN protein. Immunoblotting showed that the degradation of MYCN was accelerated by RUNX3 (Figure 4d), suggesting a negative regulation of RUNX3 on MYCN stability. As RUNX3 is a transcription factor, degradation of MYCN may be a secondary effect of the transcriptional activation mediated by RUNX3. To exclude out this possibility, we employed RUNX3-R122C, a transcriptionally incompetent mutant of RUNX3,[29,30] to test whether the transcriptional activity of RUNX3 is essential or not for the degradation of MYCN. Both RUNX3 wild type and RUNX3-R122C were able to facilitate the degradation of MYCN (Figure 4e), suggesting that the transcriptional activity of RUNX3 is not necessary. Therefore, we conclude that the protein degradation of MYCN is directly mediated by RUNX3.

RUNX3 promotes ubiquitination of MYCN, resulting in MYCN degradation

The protein stability of MYCN is regulated by a complex signaling network and the degradation of MYCN is mainly promoted by an ubiquitin-proteasome pathway.[31–33] Thus, we investigated the protein stability of MYCN in the presence or absence of proteasome inhibitor MG132. Immunoblotting showed that the overexpression of RUNX3 decreased endogenous MYCN in a dose-dependent manner, and this decrease was inhibited by an MG132 treatment (Figure 5a, left panel). This result suggests that destabilization of MYCN mediated by RUNX3 depends on the proteasomal function. Similar results were obtained in another neuroblastoma cell line NLF (Figure 5a, right panel). As the MYCN proteolysis occurs through the proteasome pathway, we asked whether ubiquitination is involved in this process. In the presence of MG132, RUNX3 efficiently facilitated the polyubiquitination of MYCN (Figure 5b, top panel). Similarly, increasing polyubiquitination of MYCN was detected in the cell lysate immunoprecipitated by anti-MYCN antibody followed by immunoblotting with anti-ubiquitin antibody (Figure 5b, bottom panel). Taken together, these results suggest that RUNX3 destabilizes MYCN through the ubiquitin-proteasome pathway.

Physical interaction between RUNX3 and MYCN

As shown above, the transcriptionally deficient mutant RUNX3-R122C can also induce the degradation of MYCN as efficiently as wild-type RUNX3, suggesting that the transcriptional activity of RUNX3 is unnecessary in this process. Therefore, we speculated that RUNX3 may directly interact with MYCN to induce its degradation. To confirm this postulation, first we examined the potential interaction between exogenous RUNX3 and MYCN. HeLa cells were transiently co-transfected with expression plasmids of MYC-tagged RUNX3 (RUNX3-MYC) and HA-tagged MYCN (HA-MYCN). Anti-MYC tag antibody precipitated RUNX3-MYC and HA-MYCN. As well, anti-HA tag antibody precipitated HA-MYCN and RUNX3-MYC, confirming that RUNX3 and MYCN could interact with each other. Furthermore, the interaction between endogenous proteins was confirmed in SK-N-BE cells (Figure 6b). As RUNX3-R122C induces the destabilization of MYCN, we also investigated whether RUNX3-R122C could bind to MYCN. We found that RUNX3-R122C co-immunoprecipitated with endogenous MYCN (Figure 6c), suggesting that the interaction between RUNX3 and MYCN is important in the process of MYCN degradation. To identify the regions of RUNX3 required for the interaction with MYCN, *in vitro* translation-coupled pulldown assay was performed (Figure 6d). Plasmids expressing a series of deletion mutants of RUNX3 protein were tranfected into HEK293 cells. Radiolabeled MYCN bound to the full length as well as several deletion constructs containing intact runt domain (deletion constructs 249, 200, Δ1-33 and Δ1-66). However, deletion constructs containing partial runt domain (Δ1-100, Δ1-133 and

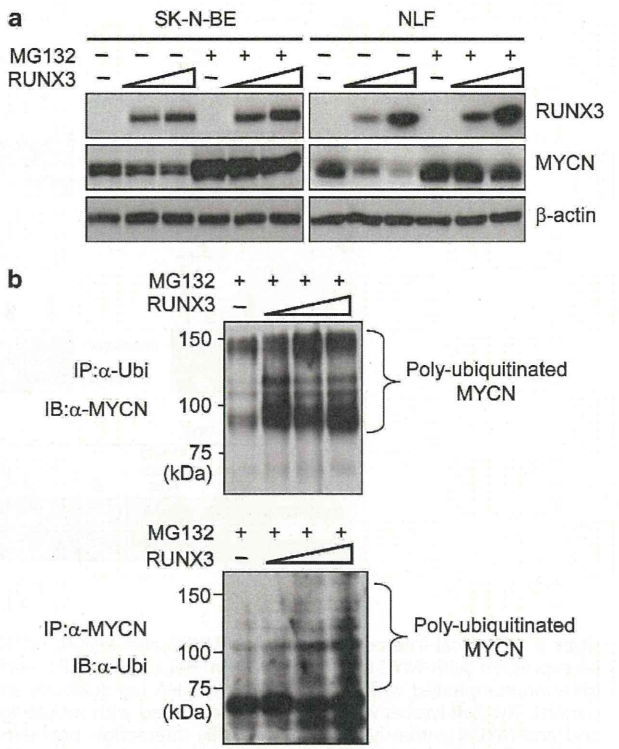

Figure 5. RUNX3 promotes ubiquitination of MYCN, resulting in MYCN degradation. (**a**) RUNX3-mediated MYCN degradation depends on proteasome function. Increasing amounts of RUNX3 expression plasmid (0, 2 and 4 μg) were transfected into SK-N-BE or NLF cells. MG132 (20 μM) was added to block proteasomal degradation. (**b**) RUNX3 induces poly-ubiquitination of MYCN. Increasing amounts of RUNX3 expression plasmid were transfected into SK-N-BE cells. Cells were treated with MG132. Whole-cell lysates were immunoprecipitated with anti-ubiquitin antibody and analyzed by immunoblotting with anti-MYCN antibody (top panel). The same cell lysates were immunoprecipitated with anti-MYCN antibody and analyzed by immunoblotting with anti-ubiquitin antibody (bottom panel). IP, immunoprecipitation; IB, immunoblotting.

Δ1-166) failed to bind to MYCN, suggesting that the N-terminal side of the runt domain is responsible for MYCN–RUNX3 interaction. Interestingly, a deletion construct fully lacking the runt domain (Δ1-200) retained the interaction capability. It was assumed that transactivation domain is also capable of MYCN interaction and the C-terminal side of the runt domain interferes it. When RUNX3-MYC and HA-MYCN were co-overexpressed, we observed colocalization of these exogenous proteins in the nucleus after 24 h of transfection, further supporting our notion (Figure 6e). Taken together, these results suggest that RUNX3 and MYCN physically interact through the runt domain of RUNX3.

RUNX3 suppresses the expression of MYCN target genes

Considering the degradation of MYCN acting as a transcription factor in neuroblastoma,[31,34] we predicted that RUNX3 may also inhibit the expression of genes targeted by MYCN. To confirm this, SK-N-BE cells were transfected with increasing amounts of RUNX3 expression plasmid. RT–PCR demonstrated that the expression levels of mRNA of MYCN-target genes, such as *MDM2*, *ID2* and *P53*,[35–37] were decreased, whereas mRNA of endogenous *MYCN* was not affected (Figure 7a). As well, overexpression of RUNX3 could overcome even exogenous MYCN to suppress the target

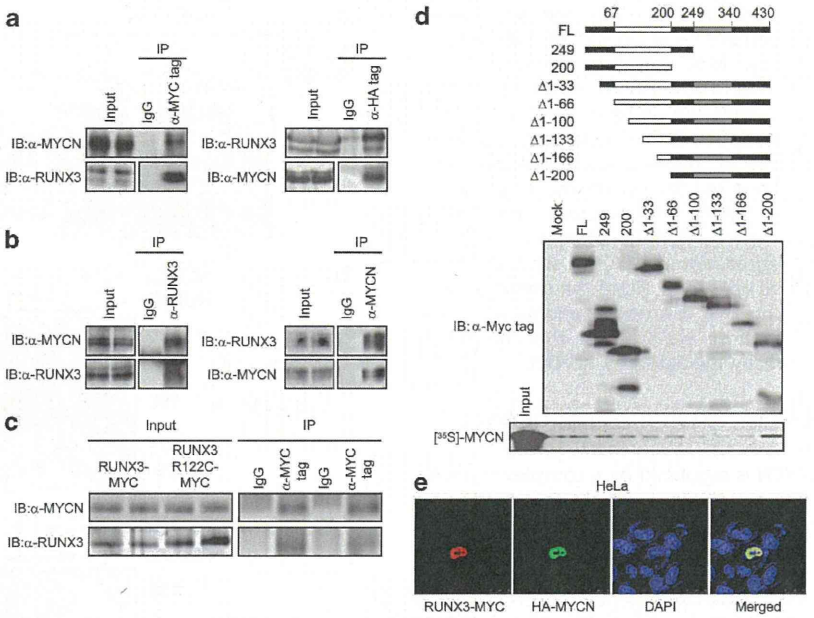

Figure 6. Physical interaction between RUNX3 and MYCN. (**a**) Exogenous MYCN and RUNX3 interact in HeLa cells. HA-tagged MYCN was co-expressed with MYC-tagged RUNX3 in HeLa cells. Cells were treated with MG132 to inhibit the MYCN degradation. Cell lysates were immunoprecipitated with mouse IgG or anti-HA tag antibody and immunoblotted with anti-MYCN antibody and anti-RUNX3 antibody (left panels). The cell lysates were immunoprecipitated with mouse IgG or anti-MYC tag antibody and immunoblotted with anti-RUNX3 antibody and anti-MYCN antibody (right panels). (**b**) Interaction between endogenous RUNX3 and MYCN. SK-N-BE cells were treated with MG132. Whole-cell lysates were subjected to immunoprecipitation with anti-RUNX3 antibody (left panels) or anti-MYCN antibody (right panels), followed by immunoblotting with anti-MYCN and anti-RUNX3 antibody, respectively. (**c**) Both RUNX3 and RUNX3-R122C interact with endogenous MYCN in SK-N-BE cells. MYC-tagged RUNX3 and MYC-tagged RUNX3-R122C expression plasmids were transfected into SK-N-BE cells. After MG132 treatment, whole-cell lysates were subjected to immunoprecipitation with anti-MYC tag antibody followed by immunoblotting with anti-MYCN and anti-RUNX3 antibody. (**d**) *In vitro* translation-coupled pulldown assay. The schematic diagram (top panel) represents full length (FL) and a series of deletion constructs of RUNX3. Runt domain (open box) and transactivation domain (shaded box) are indicated. Overexpression of FL and deletion mutants of RUNX3 in HEK293 cells were confirmed by anti-Myc tag antibody on western blotting (middle panel). ^{35}S-labeled MYCN pulled down by these RUNX3 constructs were detected by autoradiography (bottom panel). (**e**) Co-localization of RUNX3 and MYCN in the nucleus by immunofluorescent staining. HeLa cells were transfected with MYC-tagged RUNX3 (1 μg) and HA-tagged MYCN (4 μg), and were incubated with MG132. Each nucleus was visualized by 4′-6-diamidino-2-phenylindole (DAPI) staining. Exogenous RUNX3 and MYCN were detected in the nucleus by anti-MYC tag (red) and anti-HA tag (green) antibodies. Proteosome inhibitor MG132 was employed to inhibit MYCN degradation when RUNX3 was overexpressed. IP, immunoprecipitation; IB, immunoblotting.

genes (*MDM2*, *ODC1* and *CAD*) in HeLa cells (Figure 7b). Finally, we employed a couple of deletion mutants of RUNX3 (Figure 6d) to confirm the notion above. RUNX3 full length and Δ1-66 induced protein degradation of MYCN as well as suppression of MYCN-target genes, MDM2 and CAD (Figure 7c). However, unbound mutants (Δ1-100 and Δ1-200) induced neither MYCN degradation nor gene suppression. It should be noted that one of the deletion mutants (200) also failed to induce degradation and suppression, while it still binds to MYCN (Figure 6d). The deletion mutant 200 is the C-terminally truncated form of RUNX3 completely lacking the transactivation domain. As previous literatures demonstrated that this form of truncated RUNX3 lost tumor suppression capability,[38,39] we assume that this deletion mutant cannot recruit additional factors required for the MYCN degradation, even though it can interact with MYCN *in vitro*. These results clearly demonstrated that RUNX3 inhibits transcriptional activation of MYCN-target genes, suggesting that RUNX3 can block the oncogenic signaling pathway mediated by MYCN.

DISCUSSION

In this study, we found that *RUNX3* could overcome oncogenic behavior of MYCN. Consistent with our findings, *RUNX3* induces the degradation of estrogen receptor α and acts as a tumor suppressor in breast cancer.[15] Thus, we conclude that RUNX3 destabilizes oncogenic proteins, such as estrogen receptor α and MYCN, to exert its tumor-suppressive function.

Threonine 50 (T50) and serine 54 (S54) are critical amino-acid residues responsible for instability of MYCN. Initial monophosphorylation at S54 by cyclin B/cdk1 stabilizes MYCN, and primes MYCN for a second phosphorylation at T50 controlled by glycogen synthase kinase 3β. MYCN protein monophosphorylated at T50 binds to E3 ligase Fbxw7 followed by ubiquitination and degradation.[31–33,40] Early report suggested that RUNX3 transcriptionally inhibits Akt expression and therefore promotes glycogen synthase kinase 3β activation in the gastric cancer cell lines.[17] However, we did not detect the induction of glycogen synthase kinase 3β expression by RUNX3 in neuroblastoma cell line (data not shown). Rather, we showed that the transcriptionally incompetent mutant of RUNX3 could induce the degradation of MYCN, suggesting that the transcriptional activity of RUNX3 is not essential for MYCN degradation. Considering the interaction between RUNX3 and MYCN, it is possible that RUNX3 might recruit an E3 ubiquitin ligase and forms a protein complex to induce the degradation of MYCN, resulting in suppression of the transcriptional targets of MYCN. These results explain the molecular mechanism of higher survival rate observed in neuroblastoma patients in whom both *MYCN* and *RUNX3* are highly expressed. We hypothesized that high

expression of RUNX3 induces the proteasome-mediated degradation of MYCN and inhibits the MYCN oncogenic function, which contributes to the favorable outcome. In addition, as we demonstrated by cellular migration and soft agar assay, RUNX3 overexpression reduced the cellular mobility as well as anchorage-independent cell growth. As these are typical indicators of the tumor-specific property of the cell lines, it was assumed that RUNX3 overexpression improves the survival rate of the patients by inhibiting the oncogenic properties of the tumor cells.

RUNX3 is located at 1p36 where nearly 30% of neuroblastoma cases had a deletion.[3–5] Consistently, we found a positive correlation between low expression of *RUNX3* and the 1p36 loss. Although it has been reported that *RUNX3* is inactivated by hypermethylation at its promoter region in various cancers,[12–14] we did not find statistically significant correlation between the methylation status and mRNA expression levels of *RUNX3* in 110 primary neuroblastoma samples (data not shown). RUNX3 transcription factor has pivotal roles in neural development and, as far as we examined, *RUNX3* expression is very low in the majority of neuroblastoma cell lines available. Therefore, we mainly employed overexpression system, rather than knockdown strategy of *RUNX3*. Such low level of *RUNX3* could be necessary to establish the neuroblastoma cell line in which *MYCN* gene is amplified. We further assume that chromosomal 1p deletion is one of the major reasons responsible for the low *RUNX3* expression in both primary tumors and cell lines of neuroblastoma.

Taken together, we demonstrated that *RUNX3* acts as a tumor-suppressor gene in neuroblastoma. Activation of RUNX3 may suppress MYCN-mediated downstream signaling pathway. We therefore believe that the analysis of RUNX3 expression are useful for identifying low-risk neuroblastoma that are initially diagnosed as high risk and mostly increase the prognostic sensitivity.

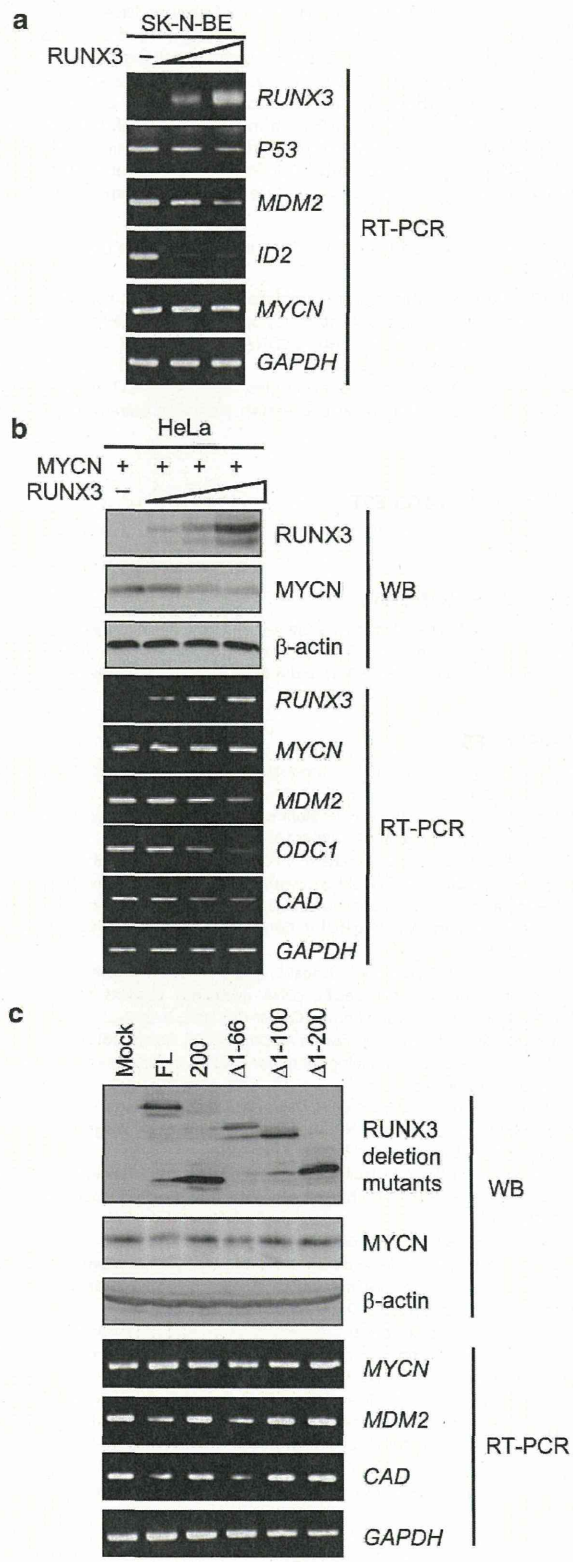

MATERIALS AND METHODS

Clinical specimens

Tumor DNA and RNA samples were obtained from 110 tumor specimens in our Neuroblastoma Resource Bank at Chiba Cancer Center Research Institute. The specimens were kindly provided from various institutions and hospitals where informed consent was obtained. All tumors were diagnosed clinically as well as pathologically as neuroblastoma and staged according to the International Neuroblastoma Staging System criteria. *MYCN* copy number, *TRKA* mRNA expression levels and DNA index were measured as reported previously.[24]

Reverse transcription–PCR and real-time PCR analyses

Total RNA was prepared from the primary neuroblastoma tissues and cell lines, followed by the first strand synthesis. RT–PCR was performed according to the manufacturer's instructions (Invitrogen, Carlsbad, CA, USA). Quantitative real-time PCR was carried out using SYBR GREEN method as the manufacturer described (Applied Biosystems, Foster City, CA, USA). Primer sequences are in the Supplementary Information.

Array-comparative genomic hybridization

Array-comparative genomic hybridization analysis was performed using UCSF BAC array (2464 BACs with 1 Mb resolution (average)) and 59 primary neuroblastomas identified as diploid were subjected to further analysis.

Figure 7. RUNX3 suppresses the expression of genes targeted by MYCN. (**a**) RUNX3 inhibits the expression of MYCN-target genes. SK-N-BE cells were transfected with RUNX3-expressing plasmid. Total RNA was used for RT–PCR. (**b**) RUNX3 inhibits the transactivation ability of exogenous MYCN. HeLa cells were co-transfected with indicated combinations of expression plasmids. Whole-cell lysates and total RNA were subjected to immunoblotting (IB; upper panels) or RT–PCR (lower panels), respectively. Actin and *GAPDH* were used as loading controls. (**c**) Unbound mutants of RUNX3 failed to induce MYCN degradation and transcriptional activation of MYCN target genes. SK-N-BE cells were transfected with indicated expression plasmids. Whole-cell lysates and total RNA were subjected to IB (upper panels) or RT–PCR (lower panels), respectively. FL, full length; WB, western blotting.

Experimental procedures and the criteria for losses and gains were described previously.[24,41]

Cell culture and transfection

The human neuroblastoma cell lines (SK-N-BE, NLF) were maintained in RPMI 1640 medium (Nissui, Tokyo, Japan) supplemented with 10% heat-inactivated fetal bovine serum (Invitrogen) and 100 mg/ml of penicillin-streptomycin (Invitrogen). HeLa and HEK293 cells were cultivated in Dulbecco's modified Eagle's medium supplemented with 10% heat-inactivated fetal bovine serum (Invitrogen) and antibiotic mixture. Transient transfection was performed using Lipofectmine 2000 transfection reagent (Invitrogen) according to the manufacturer's instructions.

Immunoblotting, immunoprecipitation and *in vitro* translation-coupled pulldown assay

For immunoblotting, cells were lysed in a lysis buffer containing 25 mM Tris-HCl, pH 7.5, 137 mM NaCl, 2.7 mM KCl, 1%Triton X-100 and protease inhibitor mixture (Sigma, St Louis, MO, USA), and spun to separate insoluble debris from the clear lysates. Equal amounts of cell lysates were separated by SDS–polyacrylamide gel electrophoresis and transferred onto Immobilon-P membranes (Milipore, Bedford, MA, USA). The transferred membranes were incubated with monoclonal anti-MYC tag (9B11, Cell Signaling Technology, Beverly, MA, USA), polyclonal anti-HA tag (561-5, MBL, Woburn, MA, USA), monoclonal anti-MYCN (Ab-1, Oncogene Research Products, Cambridge, MA, USA), polyclonal anti-MYCN (9405, Cell Signaling), polyclonal anti-actin (20–33, Sigma), monoclonal anti-RUNX3 (R3-5G4, Abcam, Cambridge, UK), monoclonal anti-ubiquitin (FK-2, Enzo, Farmingdale, NY, USA) antibodies, followed by incubation with the appropriate horseradish peroxidase-conjugated secondary antibodies (Cell Signaling Technology). For immunoprecipitation, the cell lysate of each sample contains total weight of approximately 600 μg of the protein that was extracted from 2×10^7 cells. The cell lysates were precleared with 30 μl of protein G-Sepharose suspension (Amersham Biosciences AB, Corston, UK) and then incubated with anti-MYCN monoclonal antibody or anti-RUNX3 monoclonal antibody for 2 h at 4 °C. For *in vitro* translation-coupled pulldown assay, full-length or deletion constructs of MYC-tagged RUNX3 were transfected into HEK293 cells and the cell lysate was pre-purified by MYC-tag antibody and protein G-Sepharose beads. [^{35}S] Methionine-labeled MYCN was generated in the coupled transcription/translation system (Promega, Madison, WI, USA) and mixed with pre-purified RUNX3 proteins for 2 h at 4 °C. After purification, ^{35}S-labeled bound proteins were analyzed by 10% SDS–polyacrylamide gel electrophoresis and visualized by autoradiography.

Immunofluorescence analysis

For immunofluorescence, SK-N-BE and HeLa cells were grown on coverslips and transfected with indicated expression plasmids. Forty-eight hours after transfection, cells were fixed in 100% methanol for 20 min at −20 °C, blocked in 3% bovine serum albumin, stained with the corresponding antibodies, and examined with a laser scanning confocal microscope.

Protein stability and ubiquitination assay

Cells were harvested at different time points after pretreatment with cycloheximide (100 μg/ml), and the cell lysates were employed for immunoblotting. For ubiquitination assay, SK-N-BE cells were transfected with or without RUNX3. SK-N-BE cells were exposed to the proteasomal inhibitor MG132 (20 μM) for 6 h before harvest. Cell lysates were incubated with anti-MYCN or anti-ubiquitin monoclonal antibody.

Boyden chamber assay

For the Boyden chamber assay, 50 000 pre-transfected cells were resuspended in serum-free medium and plated in the top chamber of Transwell inserts (Falcon, San Jose, CA, USA). After 24 h of transfection, cells on the bottom surface of the insert were fixed in 10% formalin and stained with a crystal violet solution. Results shown are representative of three independent experiments.

Cell proliferation assay

Pre-transfected neuroblastoma cells were seeded in 96-well plates at a density of 10^3 cells per well in a final volume of 100 μl. WST assay was performed according to the manufacturer's instruction (Cell counting Kit-8; DOJINDO, Kumamoto, Japan).

Colony formation assay

SK-N-BE cells were seeded at a final density of 500 000 cells/6 cm plate and allowed to attach overnight. Total amount of plasmid DNA per transfection was kept constant (2 μg) with pcDNA3. Forty-eight hours after transfection, cells were transferred to the fresh medium containing G418 (400 μg/ml). After 14 days, viable colonies were washed in phosphate-buffered saline and stained with Giemsa solution. For colony formation assay utilizing soft agar,[42] 2.5×10^3 cells of the RUNX3 transfected or mock transfected were seeded in triplicate in 35-mm cell culture plates containing 0.2% agar and RPMI 1640 supplemented with 10% fetal bovine serum. After 20 days, colonies with diameters >300 μm were scored as positive.

Construction of a series of deletion mutants and a point mutant of RUNX3

RUNX3 deletion mutants were amplified by PCR. PCR primers including *Eco*RI and *BamH*I restriction sites (Supplementary Information) and the amplicons were subcloned into pcDNA3.1. The point mutated RUNX3-R122C was generated utilizing the QuikChange II XL site-directed mutagenesis kit (Agilent Technologies, Loveland, CO, USA). The PCR fragments to construct these expression plasmids were verified by DNA sequencing.

CONFLICT OF INTEREST

The authors declare no conflict of interest.

ACKNOWLEDGEMENTS

This work was supported in part by a Grant-in-Aid from the Ministry of Health, Labour and Welfare for Third Term Comprehensive Control Research for Cancer, JSPS KAKENHI (Grant number 24249061) and a Grant from Takeda Science Foundation.

REFERENCES

1 Park JR, Eggert A, Caron H. Neuroblastoma: biology, prognosis, and treatment. *Hematol Oncol Clin North Am* 2010; **24**: 65–86.
2 Nakagawara A. Neural crest development and neuroblastoma: the genetic and biological link. *Prog Brain Res* 2004; **146**: 233–242.
3 Cotterill SJ, Pearson AD, Pritchard J, Foot AB, Roald B, Kohler JA *et al.* Clinical prognostic factors in 1277 patients with neuroblastoma: results of The European Neuroblastoma Study Group 'Survey' 1982-1992. *Eur J Cancer* 2000; **36**: 901–908.
4 Maris JM, Hogarty MD, Bagatell R, Cohn SL. Neuroblastoma. *Lancet* 2007; **369**: 2106–2120.
5 Ohira M, Oba S, Nakamura Y, Isogai E, Kaneko S, Nakagawa A *et al.* Expression profiling using a tumor-specific cDNA microarray predicts the prognosis of intermediate risk neuroblastomas. *Cancer Cell* 2005; **7**: 337–350.
6 Riley RD, Heney D, Jones DR, Sutton AJ, Lambert PC, Abrams KR *et al.* A systematic review of molecular and biological tumor markers in neuroblastoma. *Clin Cancer Res* 2004; **10**: 4–12.
7 Seeger RC, Brodeur GM, Sather H, Dalton A, Siegel SE, Wong KY *et al.* Association of multiple copies of the N-myc oncogene with rapid progression of neuroblastomas. *N Engl J Med* 1985; **313**: 1111–1116.
8 Suenaga Y, Kaneko Y, Matsumoto D, Hossain MS, Ozaki T, Nakagawara A. Positive auto-regulation of MYCN in human neuroblastoma. *Biochem Biophys Res Commun* 2009; **390**: 21–26.
9 Maris JM, Weiss MJ, Guo C, Gerbing RB, Stram DO, White PS *et al.* Loss of heterozygosity at 1p36 independently predicts for disease progression but not decreased overall survival probability in neuroblastoma patients: a Children's Cancer Group study. *J Clin Oncol* 2000; **18**: 1888–1899.
10 White PS, Maris JM, Beltinger C, Sulman E, Marshall HN, Fujimori M *et al.* A region of consistent deletion in neuroblastoma maps within human chromosome 1p36.2-36.3. *Proc Natl Acad Sci USA* 1995; **92**: 5520–5524.
11 Ohira M, Kageyama H, Mihara M, Furuta S, Machida T, Shishikura T *et al.* Identification and characterization of a 500-kb homozygously deleted region at 1p36.2-p36.3 in a neuroblastoma cell line. *Oncogene* 2000; **19**: 4302–4307.
12 Bangsow C, Rubins N, Glusman G, Bernstein Y, Negreanu V, Goldenberg D *et al.* The RUNX3 gene--sequence, structure and regulated expression. *Gene* 2001; **279**: 221–232.
13 Levanon D, Groner Y. Structure and regulated expression of mammalian RUNX genes. *Oncogene* 2004; **23**: 4211–4219.

14 Chuang LS, Ito Y. RUNX3 is multifunctional in carcinogenesis of multiple solid tumors. *Oncogene* 2010; **29**: 2605–2615.
15 Huang B, Qu Z, Ong CW, Tsang YH, Xiao G, Shapiro D *et al.* RUNX3 acts as a tumor suppressor in breast cancer by targeting estrogen receptor alpha. *Oncogene* 2012; **31**: 527–534.
16 Lee CW, Chuang LS, Kimura S, Lai SK, Ong CW, Yan B *et al.* RUNX3 functions as an oncogene in ovarian cancer. *Gynecol Oncol* 2011; **122**: 410–417.
17 Lin FC, Liu YP, Lai CH, Shan YS, Cheng HC, Hsu PI *et al.* RUNX3-mediated transcriptional inhibition of Akt suppresses tumorigenesis of human gastric cancer cells. *Oncogene* 2012; **31**: 4302–4316.
18 Yamada C, Ozaki T, Ando K, Suenaga Y, Inoue K, Ito Y *et al.* RUNX3 modulates DNA damage-mediated phosphorylation of tumor suppressor p53 at Ser-15 and acts as a co-activator for p53. *J Biol Chem* 2010; **285**: 16693–16703.
19 Inoue K, Ito K, Osato M, Lee B, Bae SC, Ito Y. The transcription factor Runx3 represses the neurotrophin receptor TrkB during lineage commitment of dorsal root ganglion neurons. *J Biol Chem* 2007; **282**: 24175–24184.
20 Inoue K, Shiga T, Ito Y. Runx transcription factors in neuronal development. *Neural Dev* 2008; **3**: 20.
21 Nakagawara A, Azar CG, Scavarda NJ, Brodeur GM. Expression and function of TRK-B and BDNF in human neuroblastomas. *Mol Cell Biol* 1994; **14**: 759–767.
22 Nakagawara A. Trk receptor tyrosine kinases: a bridge between cancer and neural development. *Cancer Lett* 2001; **169**: 107–114.
23 Inoue K, Ito Y. Neuroblastoma cell proliferation is sensitive to changes in levels of RUNX1 and RUNX3 protein. *Gene* 2011; **487**: 151–155.
24 Ohira M, Morohashi A, Inuzuka H, Shishikura T, Kawamoto T, Kageyama H *et al.* Expression profiling and characterization of 4200 genes cloned from primary neuroblastomas: identification of 305 genes differentially expressed between favorable and unfavorable subsets. *Oncogene* 2003; **22**: 5525–5536.
25 Nakagawara A, Arima M, Azar CG, Scavarda NJ, Brodeur GM. Inverse relationship between trk expression and N-myc amplification in human neuroblastomas. *Cancer Res* 1992; **52**: 1364–1368.
26 Nakagawara A. Molecular basis of spontaneous regression of neuroblastoma: role of neurotrophic signals and genetic abnormalities. *Hum Cell* 1998; **11**: 115–124.
27 Akter J, Takatori A, Hossain MS, Ozaki T, Nakazawa A, Ohira M *et al.* Expression of NLRR3 orphan receptor gene is negatively regulated by MYCN and Miz-1, and its downregulation is associated with unfavorable outcome in neuroblastoma. *Clin Cancer Res* 2011; **17**: 6681–6692.
28 Westermann F, Schwab M. Genetic parameters of neuroblastomas. *Cancer Lett* 2002; **184**: 127–147.
29 Chi XZ, Yang JO, Lee KY, Ito K, Sakakura C, Li QL *et al.* RUNX3 suppresses gastric epithelial cell growth by inducing p21(WAF1/Cip1) expression in cooperation with transforming growth factor {beta}-activated SMAD. *Mol Cell Biol* 2005; **25**: 8097–8107.
30 Li QL, Ito K, Sakakura C, Fukamachi H, Inoue K, Chi XZ *et al.* Causal relationship between the loss of RUNX3 expression and gastric cancer. *Cell* 2002; **109**: 113–124.
31 Gustafson WC, Weiss WA. Myc proteins as therapeutic targets. *Oncogene* 2010; **29**: 1249–1259.
32 Otto T, Horn S, Brockmann M, Eilers U, Schuttrumpf L, Popov N *et al.* Stabilization of N-Myc is a critical function of Aurora A in human neuroblastoma. *Cancer Cell* 2009; **15**: 67–78.
33 Salghetti SE, Kim SY, Tansey WP. Destruction of Myc by ubiquitin-mediated proteolysis: cancer-associated and transforming mutations stabilize Myc. *EMBO J* 1999; **18**: 717–726.
34 Fredlund E, Ringner M, Maris JM, Pahlman S. High Myc pathway activity and low stage of neuronal differentiation associate with poor outcome in neuroblastoma. *Proc Natl Acad Sci USA* 2008; **105**: 14094–14099.
35 Chen L, Iraci N, Gherardi S, Gamble LD, Wood KM, Perini G *et al.* p53 is a direct transcriptional target of MYCN in neuroblastoma. *Cancer Res* 2008; **70**: 1377–1388.
36 Lasorella A, Noseda M, Beyna M, Yokota Y, Iavarone A. Id2 is a retinoblastoma protein target and mediates signalling by Myc oncoproteins. *Nature* 2000; **407**: 592–598.
37 Slack A, Chen Z, Tonelli R, Pule M, Hunt L, Pession A *et al.* The p53 regulatory gene MDM2 is a direct transcriptional target of MYCN in neuroblastoma. *Proc Natl Acad Sci USA* 2005; **102**: 731–736.
38 Guo WH, Weng LQ, Ito K, Chen LF, Nakanishi H, Tatematsu M *et al.* Inhibition of growth of mouse gastric cancer cells by Runx3, a novel tumor suppressor. *Oncogene* 2002; **21**: 8351–8355.
39 Yano T, Ito K, Fukamachi H, Chi XZ, Wee HJ, Inoue K *et al.* The RUNX3 tumor suppressor upregulates Bim in gastric epithelial cells undergoing transforming growth factor beta-induced apoptosis. *Mol Cell Biol* 2006; **26**: 4474–4488.
40 Sjostrom SK, Finn G, Hahn WC, Rowitch DH, Kenney AM. The Cdk1 complex plays a prime role in regulating N-myc phosphorylation and turnover in neural precursors. *Dev Cell* 2005; **9**: 327–338.
41 Tomioka N, Oba S, Ohira M, Misra A, Fridlyand J, Ishii S *et al.* Novel risk stratification of patients with neuroblastoma by genomic signature, which is independent of molecular signature. *Oncogene* 2008; **27**: 441–449.
42 Takenobu H, Shimozato O, Nakamura T, Ochiai H, Yamaguchi Y, Ohira M *et al.* CD133 suppresses neuroblastoma cell differentiation via signal pathway modification. *Oncogene* **30**: 97–105.

Supplementary Information accompanies this paper on the Oncogene website (http://www.nature.com/onc)